Effects of Return Stroke Parameters and Soil Water Content on EMF Characteristics

Mohammed I. Mousa, Zulkurnain Abdul-Malek, and Mona Riza M. Esa

Institute of High Voltage and High Current, School of Electrical Engineering, Faculty of Engineering
Universiti Teknologi Malaysia, 81310, Johor Bahru, Malaysia
Mohammedimran745@yahoo.com, zulkurnain@utm.my, monariza@utm.my

Abstract ─ Electromagnetic pulses produced by lightning return strokes travel long distances both aboveground and underground. This study investigated the effects of return stroke parameters on electromagnetic propagation over lossy ground. The lightning return stroke channel was modeled using the Modified Transmission Line with Exponential Decay (MTLE) model. Electromagnetics was modeled using a frequency domain solver in the form of finite element analysis via COMSOL software. The studied stroke current parameters were peak, rise time, and decay time. In addition, the effects of soil water content was studied. Aboveground and underground electric and magnetic fields followed and were directly affected by the lightning current waveshape. The underground fields were affected by soil water content. In contrast, the aboveground fields are not affected by water content except for the radial electric field.

Index Terms ─ Current parameters, EMF, FEA, lossy ground, water content.

I. INTRODUCTION

Lightning is a vigorous natural phenomenon that has significant effects on human lives and systems such as power supply, communication, etc. Among the three lightning types, namely, cloud-to-ground, cloud-to-cloud, and intra-cloud, cloud-to-ground lightning poses the most significant threat to the above systems [1]. 90% of the cloud-to-ground lightning produces return strokes with negative current. During the last decade, many studies have calculated the electromagnetic fields radiated by these return strokes [2-5]. Ground properties are known to affect not only the lightning discharge flow in soil [6, 7] but also electromagnetic field propagation and computed fields at a given distance from the lightning source [8-12].

The two main ground properties investigated in this study were soil conductivity and permittivity. Most previous studies considered soil conductivity and permittivity as constant or frequency independent. It is noted that a correct computation of lightning electromagnetic fields requires proper soil modeling. Several soil models [7] with frequency dependency were proposed by Scott [13], Smith-Longmire [14], and Visacro-Alipio [15].

An attempt to consider frequency dependent soil conductivity and permittivity in the computation of electromagnetic fields was proposed by Delfino [16]. Delfino uses an improved numerical solver based on Maxwell equations to compute the field [16]. Later, several other researchers studied the effects of frequency dependent soil on electromagnetic fields using frequency domain solvers [17-20]. However, the full effects of lightning current magnitude, lightning current shape, and soil water content on electromagnetic field characteristics are not fully understood.

The accurate evaluation of the electromagnetic fields propagated by nearby lightning strikes is important in determining lightning induced voltage into power systems. The aim of this paper is to study the effects of lossy ground and various lightning current parameters, such as the peak, front times, and decay time, on the EMF characteristics at a given location. Finite element analysis was used for simulation. Four lightning currents with different magnitudes and shapes were considered. The effects of soil water content on EMF characteristics were also studied.

II. METHODOLOGY

The methodology of this study is comprised of four parts, namely, specification of energizing currents, modeling of the return stroke, modeling of the soil, and modeling of electromagnetic field propagation. Each of these are described below.

A. Return stroke current at base of the channel

An analytical expression was adopted to represent the lightning current at the base of the return stroke channel, as originally proposed by Heidler [21] and modified by Diendorfer and Uman. Mathematically, the return stroke current is given as $i\ (z,\ t)$, where z is the

Submitted On: May 7, 2018
Accepted On: April 3, 2019

channel height. At the bottom of the channel, the current is described as [22]:

$$i(0,t) = \frac{k_1\left(\frac{t}{\Gamma_{11}}\right)^{n_1}}{1+\left(\frac{t}{\Gamma_{11}}\right)^{n_1}} e^{\left(\frac{-t}{\Gamma_{12}}\right)} + \frac{k_2\left(\frac{t}{\Gamma_{21}}\right)^{n_2}}{1+\left(\frac{t}{\Gamma_{21}}\right)^{n_2}} e^{\left(\frac{-t}{\Gamma_{22}}\right)}, \quad (1)$$

$$\text{where} \quad k_1 = {i_{01}}/{\eta_1}, \quad k_2 = {i_{02}}/{\eta_2},$$

where i_{01} and i_{02} are the amplitudes of the current components, Γ_{11} and Γ_{12} are the front time constants, Γ_{21} and Γ_{22} are the decay-time constants, n_1 and n_2 are constants, and η_1 and η_2 are the amplitude correction factors. The corresponding values used in this study were categorized as cases 1 to 4 as shown in Table 1. Figure 1 shows the generated lightning currents for all 4 cases.

Table 1: Heidler parameters for lightning return stroke adopted from Diendorfer and Uman [22, 23]

Case	i_{01} (kA)	Γ_{11} (μs)	Γ_{12} (μs)	i_{02} kA	Γ_{21} (μs)	Γ_{22} (μs)	n_1 & n_2
1	19.5	1	2	12	8	30	2
2	17	0.4	4	8	4	50	2
3	10.5	2	4.8	9	20	26	2
4	10.7	0.25	2.5	6.5	2	230	2

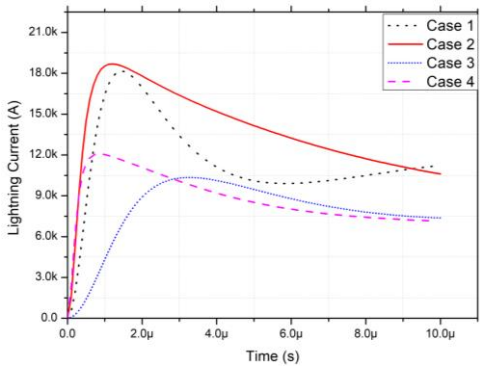

Fig. 1. Lightning current waveforms for four return stroke parameter cases (detailed parameters are given in Table 1).

B. Current distribution along the channel

Currents along the channel were implemented using the modified Transmission Line with Exponential Decay (MTLE) return stroke model. In this model, the channel base current was used to calculate currents at different channel heights. Current distribution along the channels in time domain is specified as:

$$i(z,\, t) = i(0,\, t - {z}/{v})\, e^{-\left(\frac{z}{a}\right)}, \quad (2)$$

where $i(z, t)$ is the channel current at height z, v denoted the return stroke speed, and α is the height dependent decay constant. Using a Fourier transform of $i(z, t)$ we get:

$$I(z,\, \omega) = I(0,\omega)\, e^{-\left(\frac{z}{a}\right)}\, e^{-i\omega\left(\frac{z}{v}\right)}. \quad (3)$$

Equation (3) was then used in the frequency domain solver.

C. Soil model

Based on the soil equivalent network formula of Smith and Longmire (SL) [14], the relative frequency domains permittivity and conductivity are written as:

$$\varepsilon(\omega) = \varepsilon_o\varepsilon_\infty + \varepsilon_o \sum_{i=1}^{N} \frac{a_i}{1+\left(\frac{\omega}{2\pi f_i}\right)^2}, \quad (4)$$

$$\sigma(\omega) = \sigma_o + 2\pi\varepsilon_o \sum_{i=1}^{N} \frac{a_i f_i \left(\frac{\omega}{2\pi f_i}\right)^2}{1+\left(\frac{\omega}{2\pi f_i}\right)^2}, \quad (5)$$

where,

$$\sigma_o = 8e-3\left(\frac{p}{10}\right)^{1.54}, \quad (6)$$

$$f_i = 10^{i-1}\left(\frac{p}{10}\right)^{1.28}, \quad (7)$$

where ε_∞, ε_o, and σ_o are permittivity at high-frequency, permittivity of free space, and initial conductivity, respectively. a_i and f_i are coefficients that have a good fit with the measurement results, and ω is angular frequency (with a frequency range from 100 Hz to 5 MHz). Table 2 shows a_i coefficient values for varying i values, which were used to define the soil relative permittivity and conductivity for different soil water contents.

Table 2: Coefficient a_i of Smith and Longmire expressions adopted from [14]

i	a_i	i	a_i	i	a_i	i	a_i
1	3.4E6	5	5.26E2	9	4.8	13	0.173
2	2.74E5	6	1.33E2	10	2.17		
3	2.58E4	7	2.72E1	11	0.98		
4	3.38E3	8	1.25E1	12	0.392		

Based on Smith and Longmire's soil model, soil properties can be defined for any percentage of soil water content using the initial conductivity value and f_i coefficient.

D. Electromagnetic propagation model

COMSOL software's Radio Frequency (RF-Module) was used for analysis [24] as it allows the 2D and 3D calculation of electromagnetic fields along passive and active devices. All models were based on Maxwell's equations and material laws for propagation in different media. In particular, the electromagnetic wave solver of the RF module, which is based on the finite-element solution of the weak-form representation of the frequency-domain wave equation of the magnetic vector potential [24] was used.

The electromagnetic propagation model was divided into three media channels: air, ground, and lightning. The electric parameters of air are given as σ = 0, ε_r = 1, while the ground was considered to have frequency dependent conductivity $\sigma(f)$ and relative permittivity $\varepsilon(f)$. In this model, the 2D axisymmetric formulation was utilized to model flat ground with a vertical lightning channel, and each medium was meshed

by triangular prisms based on FEA theory. Maximum element mesh sizes were limited to the skin depth δ and minimum wavelength λ_{min} (associated with maximum working frequency f_{max}). The maximum length of each element was smaller than (λ_{min}/6). To avoid large computational requirements and inefficient matrix systems in the FEM formulation due to large model dimensions, a thin wire was used to represent the lightning channel. The conductor wire was reasonably modeled as a sequence of mesh edges [17, 20] with a maximum edge length of (λ_{min}/10).

Electromagnetic wave and frequency domain interfaces were used to solve time-harmonic electromagnetic field distribution. This physics interface solved the second-order vector wave equation for electric fields [21]:

$$\nabla \times (\mu_r^{-1} \nabla \times E) - \frac{\omega^2}{c^2} \left(\varepsilon_r - j\frac{\sigma}{\omega\varepsilon_0}\right) E = 0, \quad (8)$$

while the magnetic field was determined using the first Maxwell equation:

$$\nabla \times E = -j\omega\mu_r\mu_o H, \quad (9)$$

where E, and H are the electric and magnetic fields. The variables μ_r, ε_r, and σ are relative permeability, relative permittivity, and electric conductivity, respectively; ω is angular frequency, c is propagation speed of light, and $\nabla\times$ is the curl of the vector variables.

In COMSOL, the soil–air interface used natural Neumann conditions expressed as:

$$-n \times [(\mu_r^{-1} \nabla \times E)_{Soil} - (\mu_r^{-1} \nabla \times E)_{Air} = n \times j\omega\mu_o(H_{Soil} - H_{Air}) - J_s = 0, \quad (10)$$

where E_{Soil} and E_{Air} are the electric fields at the soil–air interface, H_{Soil} and H_{Air} are the magnetic fields at the same interface, J_s denotes surface current density, and n is the unit normal vector directed from soil to air. To prevent the electromagnetic wave from being reflected off of boundaries, a Perfect Match Layer (PML), (available in the frequency domain RF module) was used. PML width is equal to (2 λ_{min}) [24].

The electromagnetic field radiated by the lightning channel is defined by three components, the vertical electric field (E_z), the radial electric field (E_r), and the azimuthal magnetic field (H_ϕ). The electromagnetic component was obtained in the time domain using the inverse Fourier transform.

Table 3 lists the parameters used to calculate current along a lightning channel and other simulation details [17]. Figure 2 shows the FEA simulation model consisting of lightning channels for the ground, air, and Perfectly Matched Layers as well as the generated FEA mesh.

Figure 3 illustrates the flow chart of the computational procedure for modeling the electromagnetic propagations over lossy ground.

Table 3: Parameters used for return stroke model and electromagnetic computation

Parameters/Symbols	Values
Return stroke speed v, [m/s]	1.3 x 10^8
Range of frequency f, [Hz]	(0 – 5 x 10^6)
Number of samples	1024
Lambda λ, [m]	60
Decay constant α, [m]	2000
Max. Mesh size, [m]	(λ/f_{max}) = 30
Min. Mesh size, [m]	0.07
Height of lightning channel [m]	7000
Width of the model [m]	4500
Depth of ground [m]	1000

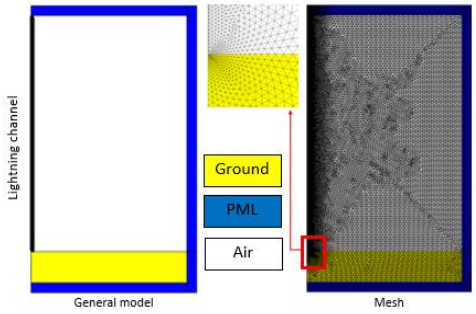

Fig. 2. Lightning channel and electromagnetic model containing ground, air, and Perfectly Matched Layers (PML) as well as the generated FEA mesh.

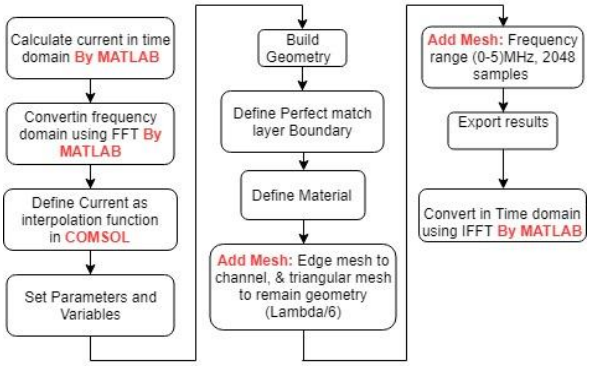

Fig. 3. Flow chart of the numerical solution.

III. RESULTS AND DISCUSSION

This study simulated the effects of lightning current parameters and soil water content on computed electromagnetic fields.

A. Effects of lightning current parameters

Figure 4 shows the resultant radial and vertical components of the electric field and the azimuthal

component of the magnetic field for lossy ground for four lightning return stroke currents. The observation point was located 10 m above ground and 50 m from the lightning channel. It was observed that the measured aboveground electric and magnetic fields followed and were directly affected by the lightning current waveshape. With proper calibration, the measurement of these aboveground fields enables us to determine the magnitude and shape of a lightning current source.

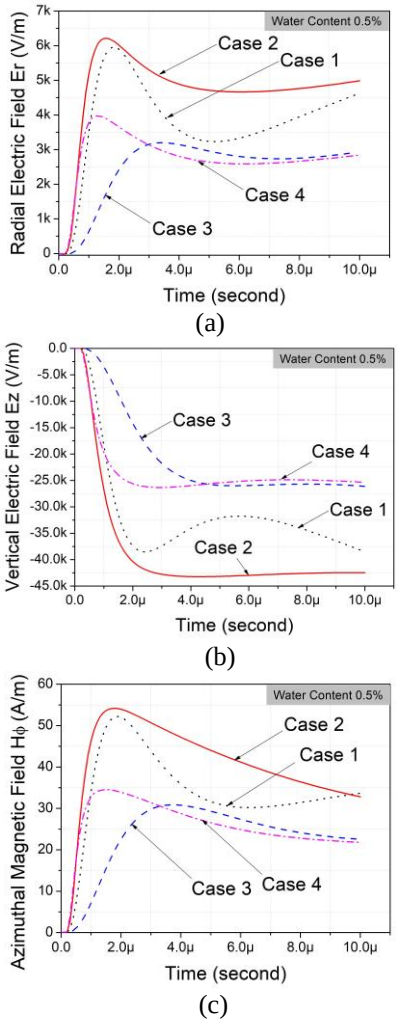

Fig. 4. Variation of electromagnetic components over lossy ground for: (a) Radial component of the electric field (E_r), (b) vertical component of the electric field (E_z), and (c) azimuthal component of the magnetic field (H_ϕ).

Figure 5 shows the effect of lossy ground on the radial and vertical electric fields and the azimuthal magnetic field for all lightning return stroke currents. The observation point was located 10 m belowground and 50 m from the lightning source. It was observed that the measured underground radial electric and magnetic fields followed and were directly affected by the lightning current waveshape. Similar to the aboveground case, the measurement of these two underground fields enables us to determine the magnitude and shape of a lightning current source.

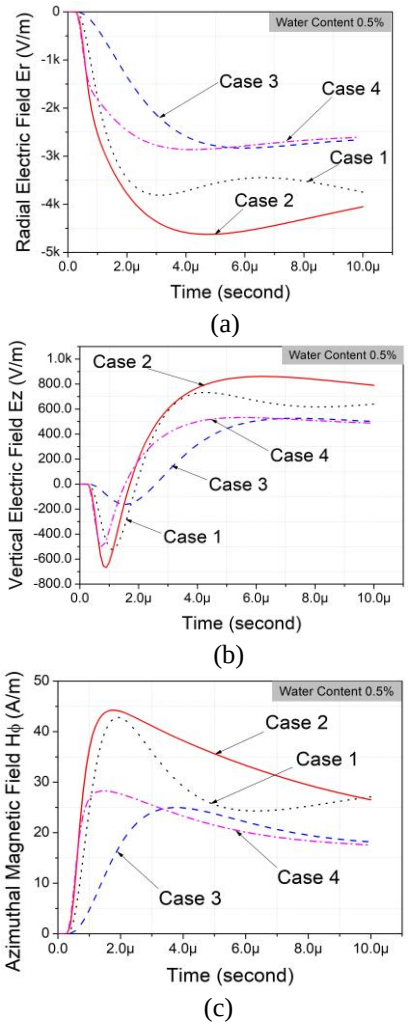

Fig. 5. Variation of electromagnetic components in lossy ground for: (a) Radial component of the electric field (E_r), (b) vertical component of the electric field (E_z), and (c) azimuthal component of the magnetic field (H_ϕ).

B. Water content effect

Figure 6 shows radial electric fields with water content for return stroke currents at locations 50 m from the lightning channel and 10 m above and below ground. It was observed that the water content impacted the underground currents magnitude and the pattern of the radial electric field until 10% soil water content. For water content above 10%, the field magnitude was approximately zero. Water content (up to 10%) increased the aboveground field. Increment amounts were dependent on current shape.

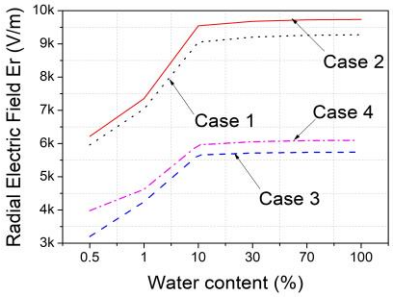

(a)

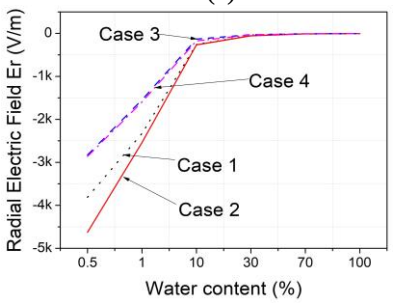

(b)

Fig. 6. Peak radial electric fields with water content for four return stroke cases 50 m from the lightning channel at: (a) 10 m aboveground and (b) 10 m below ground.

Figure 7 shows variations in the above and underground vertical electric fields with water content for four return stroke currents 50 m from the lightning channel. It was observed that the water content impacted the underground currents magnitude and the pattern of the vertical electric field until about 10% soil water content. For water content above 10%, the field magnitude was approximately zero. Unlike the radial field, water content did not affect the aboveground vertical field.

Figure 8 shows variations in above and underground azimuthal magnetic fields with water content for four current cases 50 m from the emitting source. It was observed that the underground magnetic field linearly decreased when increased water content from 1 to 100%. The decrement amount depended on current shape. For the vertical electric fields, the aboveground magnetic field remained unaffected by water content.

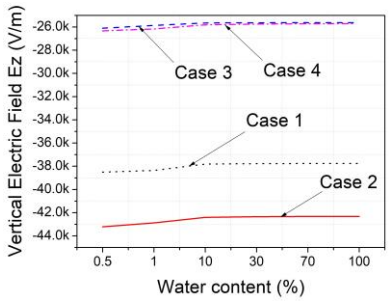

(a)

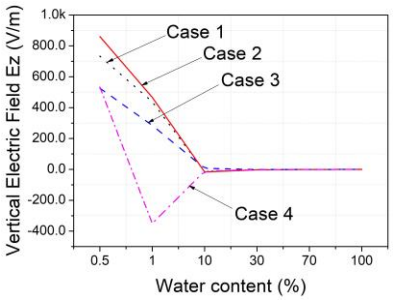

(b)

Fig. 7. Vertical electric fields with water content for four return strokes determined 50 m from the lightning channel at: (a) 10 m aboveground and (b) 10 m belowground.

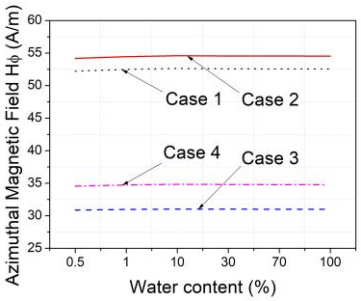

(a)

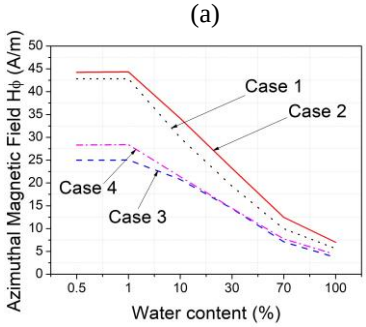

(b)

Fig. 8. Azimuthal magnetic fields with water content for four return strokes determined 50 m from the lightning channel at: (a) 10 m aboveground and (b) 10 m belowground.

Results showed that the waveforms of the electric and magnetic fields have similar patterns to the return stroke current waveform above/belowground, with the exclusion of underground vertical electric field. Hence, the waveform shape for the vertical electric field was mainly affected by soil conductivity frequency dependency [17].

For all return stroke cases, the peak value and pattern of the three electromagnetic components behaved differently due to soil electrical parameters. Hence, the peak values of the radial electric field increased with increased soil conductivity and decreased

permittivity (higher water content according to [14]). In contrast, the underground fields were dampened, especially for soil water contents greater than 10%. The peak values for underground vertical electric fields were significantly affected by soil electric parameters. The aboveground fields were unaffected by increased water content. Differences were found in the behavior of peak values between return strokes.

Simulation results were based on the electromagnetic model presented by Akbari [17] and different solver techniques in [16, 19]. The electric and magnetic fields results of case 4 are in good agreement with those presented in [16, 17] for both above/ belowground for various distances from the lightning channel. Using case 4 as reference, other cases were evaluated over different soils.

IV. CONCLUSION

The shape and magnitude of above and belowground electric and magnetic fields were directly affected by the lightning current waveform. The measurement of the lightning electric and magnetic field waveforms enables us to determine the magnitudes and shape of a lightning currents source. Underground fields were found to be affected by 0.5% to 100% soil water content. The effect was more dominant for the azimuthal magnetic field (up to 100% water content) compared to the radial and vertical electric fields, which were only affected by up to 10% soil water content. In contrast, aboveground fields were not affected by soil water content, except for the radial electric field (up to 10% water content).

Soil water content had various effects on electromagnetic component peak values for the four return strokes. There was no significant differences in the effect of water content for the aboveground return strokes. For the underground fields, all three electromagnetic components behaved slightly different at different soil water contents. Electric fields were almost constant after 10% of water content, while the magnetic field continually decreasing with increases in water content up to 100%.

ACKNOWLEDGMENT

The authors wish to thank the Ministry of Education (MOE) and Universiti Teknologi Malaysia (Research Nos. 4F828 and 18H10) for the financial aid.

REFERENCES

[1] V. Cooray, "Return stroke models for engineering applications," in *Lightning Electromagnetics*, London, United Kingdom: The Institution of Engineering and Technology, 2012.

[2] C. Y. Wang, W. Haojiang, and W. Lipeng, "Characteristics of lightning electromagnetic fields from oblique lightning channel considering vertical stratified ground," *JEIT*, vol. 39, pp. 466-473, 2017.

[3] M. O. Goni, E. Kaneko, and A. Ametani, "Simulation of lightning return stroke currents and its effect to nearby overhead conductor," *Applied Computational Electromagnetics Society Journal*, vol. 24, no. 5, pp. 469-477, 2009.

[4] Y. Baba and M. Ishii, "Characteristics of electromagnetic return-stroke models," *IEEE Transactions on Electromagnetic Compatibility*, vol. 45, pp. 129-134, 2003.

[5] V. Rakov, "Characterization of lightning electromagnetic fields and their modeling," in *14th Int. Zurich Symposium on Electromagnetic Compatibility*, pp. 3-16, 2001.

[6] M. I. Mousa, Z. Abdul-Malek, V. M. Ibrahim, A. I. Elgayar, Z. Nawawi, and M. A. Sidik, "Evaluation and mitigation of underground gas pipeline coating stress due to nearby lightning stroke," in *Electrical Engineering and Computer Science (ICECOS), 2017 International Conference on*, pp. 275-279, 2017.

[7] M. O. Goni, E. Kaneko, and A. Ametani, "Simulation of lightning return stroke currents and its effect to nearby overhead conductor," *Applied Computational Electromagnetics Society Journal*, 24.5: pp. 469-477, 2009.

[8] M. Mokhtari, Z. Abdul-Malek, and C. L. Wooi, "Integration of frequency dependent soil electrical properties in grounding electrode circuit model," *International Journal of Electrical and Computer Engineering*, vol. 6, pp. 792, 2016.

[9] N. Rameli, M. Z. A. Ab-Kadir, M. Izadi, C. Gomes, and N. Azis, "Variations in return stroke velocity and its effect on the return stroke current along lightning channel," in *2016 33rd International Conference on Lightning Protection (ICLP)*, pp. 1-5, 2016.

[10] M. Izadi, M. A. Ab Kadir, and M. Hajikhani, "Evaluation of lightning current and ground reflection factor using measured electromagnetic field," *Applied Computational Electromagnetics Society Journal*, vol. 29.1, 2014.

[11] D. Li, M. Azadifar, F. Rachidi, M. Rubinstein, M. Paolone, D. Pavanello, et al., "On lightning electromagnetic field propagation along an irregular terrain," *IEEE Transactions on Electromagnetic Compatibility*, vol. 58, pp. 161-171, 2016.

[12] K. Arzag, Z. Azzouz, and B. Ghemri, "Lightning electromagnetic pulse simulation using 3D-FDTD method (Comparison between PEC and UPLM Boundary Conditions)," in *Lightning Protection (ICLP)*, 2016 33rd International Conference on, pp. 1-6, 2016.

[13] J. Scott, R. Carroll, and D. Cunningham,

"Dielectric constant and electrical conductivity of moist rock from laboratory measurements," *US Dept. of Interior Geological Survey Technical Letter*, Special projects-12, vol. 17, Aug. 1964.

[14] C. L. Longmire and K. S. Smith, "A universal impedance for soils," *Mission Research Corp*, Santa Barbara, CA, 1975.

[15] S. Visacro and R. Alipio, "Frequency dependence of soil parameters: Experimental results, predicting formula and influence on the lightning response of grounding electrodes," *IEEE Transactions on Power Delivery*, vol. 27, pp. 927-935, 2012.

[16] F. Delfino, R. Procopio, M. Rossi, and F. Rachidi, "Influence of frequency-dependent soil electrical parameters on the evaluation of lightning electromagnetic fields in air and underground," *Journal of Geophysical Research: Atmospheres*, vol. 114, 2009.

[17] M. Akbari, K. Sheshyekani, A. Pirayesh, F. Rachidi, M. Paolone, and A. Borghetti, "Evaluation of lightning electromagnetic fields and their induced voltages on overhead lines considering the frequency dependence of soil electrical parameters," *IEEE Transactions on Electromagnetic Compatibility*, vol. 55, pp. 1210-1219, 2013.

[18] K. Sheshyekani and M. Akbari, "Evaluation of lightning-induced voltages on multiconductor overhead lines located above a lossy dispersive ground," *IEEE Transactions on Power Delivery*, vol. 29, pp. 683-690, 2014.

[19] F. H. Silveira, S. Visacro, R. Alipio, and A. De Conti, "Lightning-induced voltages over lossy ground: The effect of frequency dependence of electrical parameters of soil," *IEEE Transactions on Electromagnetic Compatibility*, vol. 56, pp. 1129-1136, 2014.

[20] S. Visacro and F. H. Silveira, "The impact of the frequency dependence of soil parameters on the lightning performance of transmission lines," *IEEE Transactions on Electromagnetic Compatibility*, vol. 57, pp. 434-441, 2015.

[21] F. Heidler, "Traveling current source model for LEMP calculation," *in Proc. 6th Int. Zurich Symp. Electromagn. Compat.*, pp. 157-162, 1985.

[22] V. A. Rakov and M. A. Uman, "Review and evaluation of lightning return stroke models including some aspects of their application," *IEEE Transactions on Electromagnetic Compatibility*, vol. 40, pp. 403-426, 1998.

[23] M. Izadi, A. Kadir, M. Z. Abidin, C. Gomes, and W. F. Ahmad, "An analytical second-FDTD method for evaluation of electric and magnetic fields at intermediate distances from lightning channel," *Progress in Electromagnetics Research*, vol. 110, pp. 329-352, 2010.

[24] R. Comsol, *Module User's Guide*, Ed: Version: May, 2012.

Mohammed I. Mousa received the B.Sc. degree in Power Electrical Engineering from Al-Furat Al-Awsat Technical University, Babil, Iraq, in 2010, the M.E. degree in Electrical Engineering from the Universiti Teknologi Malaysia, Johor, Malaysia, in 2014, and is currently pursuing the Ph.D. degree in Electrical Engineering at the Institute of High Voltage and High Current (IVAT), Universiti Teknologi Malaysia. His research interest include the high voltage engineering, the power system transient simulation, and lightning phenomena.

Z. Abdul-Malek received the B.E. degree in Electrical and Computer Systems from Monash University, Melbourne, Australia, in 1989, the M.Sc. degree in Electrical and Electromagnetic Engineering with Industrial Applications from the University of Wales Cardiff, Cardiff, U.K., in 1995 and the Ph.D. degree in High Voltage Engineering from Cardiff University, Cardiff, U.K., in 1999. He was a Lecturer with Universiti Teknologi Malaysia (UTM) for 29 years, where he is currently a Professor of High Voltage Engineering with the Faculty of Electrical Engineering. He is currently the Director of the Institute of High Voltage and High Current (IVAT), UTM.

M.R.M. Esa received the B.E. degree in Electrical-Telecommunication in 2003 and the Master degree in Electronic-Telecommunication in 2005 from Universiti Teknologi Malaysia (UTM), in 2005. In 2014, she received the Ph.D. degree with a specialization in atmospheric discharges and lightning physics from Uppsala University, Sweden. Currently, she is a Senior Lecturer at the Faculty of Engineering and the Head of High Voltage Laboratory in UTM.